Photopolymerized Cross-Linked Polyacrylamide Gels for On-Chip Protein Sizing

Amy E. Herr, Anup K. Singh
Biosystems Research Department, Sandia National Laboratories, Livermore, CA 94551
aeherr@sandia.gov

Abstract

In this work, a new method for on-chip sodium dodecyl sulfate polyacrylamide gel electrophoresis (SDS-PAGE) of proteins is reported. Miniaturization of SDS-PAGE has attracted significant attention as it offers rapid analysis times, excellent resolution, high throughput, and the potential for integration and automation, as compared to conventional counterparts. The presented on-chip SDS-PAGE technique employed photolithographically patterned, cross-linked gels fabricated *in situ* in less than 20 minutes. The effects of sieving gel composition on the migration properties of fluorescently labeled protein standards (ranging in molecular weight from 14.2 to 66 kDa) were quantified, as was the ability of the gels to function as a sieving matrix for biologically relevant species. Ferguson analysis was employed to calculate retardation coefficients and free solution mobilities. In conjunction with fluorescence imaging, the on-chip SDS-PAGE separation mechanism was evaluated in terms of separation performance indices, as well as limiting behaviors (i.e., free solution mobility, exclusion characteristics). The photolithographically fabricated gels employed for on-chip SDS-PAGE allowed rapid (< 30 s) separations of proteins in short separation lengths (4 mm) with efficiencies as high as 4.41 x 10^5 plates per meter. The on-chip SDS-PAGE separations were ~100 times faster than conventional slab gel SDS-PAGE (60 min) and occurred in a fraction of the separation length required by the slab gel. The migration

behavior of protein standards correlated well with molecular weight and allowed molecular weight determination for interleukin-2, fibroblast growth factor, insulin like growth factor, and tetanus toxin C-fragment.

Introduction

Analysis of protein function and identification of proteins for use as diagnostic or therapeutic markers relies upon methods for quantitating species present in complex sample mixtures. Sodium dodecyl sulfate polyacrylamide gel electrophoresis (SDS-PAGE) has proven to be the standard for such analyses.[1-3] Electrophoresing SDS-protein complexes through a sieving matrix allows separation of species based exclusively on size, since denaturing and reducing proteins in the presence of SDS results in similar charge-to-mass characteristics for most protein species. SDS-PAGE thus provides a means to perform efficient separations over short distances. Combining SDS-PAGE with isoelectric focusing further extends the resolving power of the techniques.[4] While slab gel SDS-PAGE is effective, the technique is slow and labor-intensive. In an effort to address these drawbacks, SDS-PAGE has been adapted for use in capillary[5-8] and microdevice formats.[9-12] Both formats have improved the required analysis times, increased the potential for automation, and reduced integration complexity.

The performance of electrophoretic separation systems can be greatly enhanced using microfabricated formats.[13-15] The small length scales associated with microdevice geometries enable precise definition of minute sample plugs, minimizing separation distances and times. For microdevice-based SDS-PAGE applications, non-cross-linked polymer matrices have been used with success.[9, 10] Cross-linked polymer matrices, when

used in conjunction with photolithographic fabrication process, have the potential to enable high-resolution patterning of localized functionality within the microdevice. Photodefined cross-linked polymers have been shown to perform well for on-chip DNA sizing[16], DNA and protein localization[17-21], and chromatography.[22-24] Direct adaptation of slab gel SDS-PAGE, which relies on a cross-linked sieving matrix, to a chip-based format necessitates use of an *in situ* gel fabrication technique. The nature of cross-linked gels renders introduction of an *ex situ* fabricated gel into a microfluidic device troublesome. In addition, photolithographically patterned soft polymers[25, 26] offer numerous advantages to on-chip SDS-PAGE: faster curing times as compared to chemically polymerized gels, easier fluid handling than high viscosity bulk polymer solutions, facile tailoring of the sieving matrix porosity for specific applications, and improved separation resolution arising from prevention of non-specific protein adsorption on separation channel walls.[27] Utilizing these advantages, *in situ* fabricated polymer matrices could further aid development of complex, integrated chip-based systems, such as multi-dimensional separation schemes.[25, 28-31]

In this work, we present a method for protein sizing based on use of photodefined cross-linked polyacrylamide gels in a microfabricated analytical device. Fluorescently labeled proteins are separated by on-chip SDS-PAGE in an effort to investigate the effects of various gel compositions on device performance. Full-field CCD imaging is used as a tool for characterization of the technique. Limiting behaviors and trends observed during the separations are used to validate the separation mechanism governing the on-chip SDS-PAGE technique. Finally, the on-chip SDS-PAGE technique is applied to the sizing and separation of biologically relevant species.

Experimental Section

Chemicals. The water-soluble photoinitiators 2,2'-Azobis(2-methylpropionamide)dihydrochloride (V-50) and 2,2'-Azobis[2-methyl-N-(2-hydroxyethyl)propionamide] (VA-086) were purchased from Wako Chemicals (Richmond, VA). Solutions of 3-(trimethoxysilyl)propyl methacrylate (98%), 40% acrylamide, and 30% (37.5:1) acrylamide/bis-acrylamide were purchased from Sigma (St. Louis, MO). Premixed 10x tris/glycine/SDS electrophoresis buffer (25 mM Tris, pH 8.3, 192 mM glycine, 0.1% SDS) was purchased from BioRad (Hercules, CA). Deionized water (18.2 MΩ) was obtained using an Ultrapure water system from Millipore (Milford, MA).

Protein Samples. Molecular weight markers (Sigma) consisted of five fluorescently labeled species in solution (62mM Tris, 1mM EDTA, 3% sucrose, 0.5% dithiothreitol, 2% SDS and 0.005% bromphenol blue). The markers included: aprotinin (bovine lung), MW 6.5 kDa; α-lactalbumin (bovine milk), 14.2 kDa; trypsin inhibitor (soybean), 20.1 kDa; carbonic anhydrase (bovine erythrocyte), 29 kDa; alcohol dehydrogenase (horse liver), 39 kDa; and bovine serum albumin, 66 kDa and were prepared for on-chip SDS-PAGE per instructions from the supplier (heating to 65°C for 5 minutes). Note that the absolute concentration of each protein in the stock solution is unknown, and consequently, protein concentrations are quoted relative to the stock solution. Prior to use, stock samples were diluted in tris/glycine/SDS run buffer by a factor of 3x. The proteins α-lactalbumin, trypsin inhibitor, carbonic anhydrase, and alcohol dehydrogenase

were used as sizing standards for all gel concentrations in this work, bovine serum albumin was additionally used in the 6% gels, and aprotinin did not consistently provide a sufficient signal-to-noise ratio to be used as a standard.

Recombinant tetanus toxin C-fragment (TTC, the atoxic binding portion of the native tetanus toxin[32], MW 51.9 kDa) was purchased from Roche (Indianapolis, IN). Recombinant human interleukin-2 (IL-2, MW 15.5), recombinant human fibroblast growth factor-basic (FGF, MW 17.4), and recombinant human insulin like growth factor-I (IGF, MW 7.7) were purchased from ProSpec-Tany TechnoGene LTD (Rehovot, Isreal). Alexa Fluor 488 protein labeling kits were purchased from Molecular Probes (Eugene, OR). IL-2, FGF, and IGF were fluorescently labeled with Alexa Fluor 488 per instructions provided in the product information accompanying the fluorescent labeling kit (Molecular Probes Product Sheet 10235). Fluorescein isothiocyanate (FITC) was reacted with TTC to form the fluorescent TTC* species using a standard protocol (Molecular Probes Product Sheet 06434). All fluorescently labeled species were stored at 5°C in the dark until use. Protein samples were denatured by mixing 2:1 with denaturing buffer (4% SDS and 3% β-mercaptoethanol) and heated to 85°C for 5 min. Post-labeled protein concentrations were estimated to be in the low micromolar range.

Chip Fabrication. As previously described,[24] standard photolithography, wet etching, and bonding techniques were used to fabricate the microchips from Schott D263 glass wafers (4-in. diameter, 1.1-mm thickness; S. I. Howard Glass Co. Worcester, MA). The chips used for SDS-PAGE consisted of offset double-T junctions having injection arms and a buffer arm that each measured 0.5 cm in length (Figure 1). The channels were ~40

μm deep x ~100 μm wide. Depending on the device, separation channel lengths were either 6.1 cm or 6.7 cm. After fabrication and bonding, the quality of the microchannels was visually assessed using a microscope. Nanoport assemblies from Upchurch Scientific (Oak Harbor, WA) were used as buffer reservoirs.

Chip Preparation. Microchannels were prepared for polyacrylamide gel polymerization using a two-step channel coating procedure similar to that described by Kirby *et al*.[33] First, microchannels were functionalized using acrylate-terminated self-assembled monolayers. Subsequently, the microchannels were coated with linear polyacrylamide. Acrylamide is a neurotoxin absorbed through the skin. Proper handling procedures are required. Channels were cleaned by an initial 10 min 1M NaOH flush, followed by a 10 minute deionized water rinse and an air purge of the channels. A 2:3:5 mixture of 3-(trimethoxysilyl)propyl methacrylate, glacial acetic acid, and deionized water was used for channel conditioning. The mixture was subjected to a 5 min sonication and degassing step, after an initial vigorous mixing step (during addition of the water) that ensured all constituents were in solution. At the end of the 30-minute conditioning step, the channels were purged with air in an effort to reduce the chance of channel clogging. Following these steps, the channels were rinsed with deionized water for 10 minutes. A solution of 5% (*w/v*) acrylamide containing 5 mg/mL V-50 was flushed through the channels. Channels filled with the acrylamide coating solution were exposed to a 100 W mercury lamp for 10 minutes resulting in formation of a linear polyacrylamide channel coating. The lamp was fan-cooled to minimize heating. Following the coating procedure, chips were flushed with deionized water for 5 minutes and stored filled with water at 5°C.

Following surface preparation, polyacrylamide gels of various total acrylamide concentrations (monomer plus cross-linker) were fabricated in the microdevices. *n*% (*n* = 4, 6, 8, and 10, where *n* is the total acrylamide concentration) polyacrylamide gel matrixes were fabricated by adjusting the total volume of the 30% acrylamide/bis-acrylamide solution with tris/glycine/SDS run buffer containing 0.2% (*w/v*) VA-086 photoinitiator. Figure 1A-D schematically depicts the polymer fabrication steps. Briefly, all conditioned channels in a device were filled with the unpolymerized acrylamide solution using a low flow rate pressure-driven flow, as shown in Figure 1A and B. In some instances, portions of the microdevice were masked using a UV blocking material (e.g., masking film such as Rubylith, electrical tape) to prevent photopolymerization of those channels as depicted in Figure 1C. In all work presented here, no masking was employed; thus, all channels were exposed to a 4 W UV illumination source (λ = 365 nm) for 15 minutes. An additional 3 minutes of UV exposure was required for full polymerization of gel-filled channels near multiple inlet channels (i.e., regions near a t-junction). Voids or 'tears' form near the offset double-T junction upon application of an electric field if this extended photopolymerization step is omitted. The tears may arise from stresses induced by electroosmotic flow in channels filled with a non-uniformly polymerized gel.[21] As depicted in Figure 1D, the UV exposure step resulted in localization of a cross-linked gel matrix in unmasked device regions. Chips containing polyacrylamide structures were stored submerged in buffer solution and refrigerated at 5°C.

Apparatus and Imaging. Sample introduction and separation were performed using common electrokinetic injection methods. The sample waste (SW), buffer (B), and waste

(W) reservoirs on a standard offset double-T microdevice were filled with the tris/glycine/SDS run buffer (Figure 1). The sample (S) reservoir was filled with the sample solution. A programmable high-voltage power supply, designed and fabricated in-house, provided voltage control and current monitoring at platinum wires which served as electrodes. Samples were loaded by applying a +300 V potential at the SW reservoir and grounding the S reservoir for ~1 minute (E = 300 V/cm). During loading, both the B and BW reservoirs were grounded to form a 'pinched' injection plug. To perform an SDS-PAGE separation, +1820V was applied at the BW reservoir while grounding the B reservoir (i.e., the electrophoretic mobility of the proteins dominates the electroosmotic mobility in the channel). During the separations both the S and SW reservoirs were allowed to electrically float. No 'pull-back' voltage was necessary, as the high fluidic resistance of the polymer matrix reduced leakage of sample from the loading arms into the separation channel. As implemented, the polyacrylamide gel is reusable, thus a single gel was used to analyze multiple sample mixtures. To reduce the risk of cross-contamination between samples, fresh tris/glycine/SDS buffer was electrokinetically flushed through all device channels for 5-7 minutes after final SDS-PAGE analysis of a given sample mixture.

The species transport was observed using standard epifluorescence microscopy techniques and digital image collection. A 1300 × 1030, Peltier-cooled interline CCD camera (CoolSnap HQ, Roper Scientific, Trenton NJ) was employed for image collection. Pixel binning (1x2 or 4x4) and region of interest selection were employed, thus allowing an image-sampling rate of up to 5 Hz. Images were collected using an inverted epifluorescence microscope (IX-70, Olympus, Melville, NY) equipped with 4×

and 10× objectives (numerical apertures of 0.16 and 0.4, respectively). An *x*-*y* translation stage (Olympus, Melville, NY) was used to position the chip and fixturing relative to the imaging optics. A 0.31× demagnifier (Diagnostic Instruments Inc., Sterling Heights, MI) was used to increase the field of view projected onto the CCD. Image analysis was conducted using available and in-house Java plug-ins developed using ImageJ (National Institutes of Health, Bethesda, MD, http://rsb.info.nih.gov/ij/). Images were corrected for background signal to adjust for spatial non-uniformities in the excitation and collection efficiencies.

Quantifying Performance. The separation resolution, *SR* was employed as a measure of separation performance in assays where spatial concentration distributions were obtained through full-field CCD imaging. The SR performance metric was calculated using the relationship[34] $SR = \Delta L/w$, where ΔL is peak-to-peak distance between analyte bands of interest and w is a measure of analyte band width (in this work w indicates the full width half maximum of the concentration distribution). Electropherograms (intensity *vs.* time) were obtained using the CCD camera as a virtual single-point detector. In single point detection mode, the CCD pixels were binned to form super-pixels and intensity information at a single location was recorded as a function of time. For data acquired using this imaging mode, separation performance was quantified using the relationship $N = 5.54 \times (t/\Delta t_{1/2})^2$, where t is the migration time and $\Delta t_{1/2}$ is the peak full width at half maximum (using a Gaussian distribution, $\Delta t_{1/2} \sim 2.35\sigma$). N/m and N/s were calculated by dividing N by the distance to the detector and by the elution time, respectively.

Results and Discussion

Performance of *in situ* Photopolymerized Gels. An SDS-PAGE separation of the molecular weight standards is shown in Figure 1E. The CCD image was taken after an elapsed separation time of 6.4 s (E = 298 V/cm, 6% polyacrylamide gel matrix). Near baseline resolution of the proteins was achieved in a 5 mm separation length. As the focus of this work centers on attaining rapid separations in a short separation distance, N/m emerges as a relevant performance metric.[34] For the separation conditions presented in Figure 1E, N/m based on peak 2 is 3.97×10^5, which compares favorably with slab gel single percentage SDS-PAGE (N/m ~2.94×10^5 for a 10% gel). The short separation distances, and associated rapid separation times, arise mainly from the small-injected analyte plug widths realizable using the microsystem format.[35] The separations characterized here employed a 'pinched' injection scheme with channel injector offsets of 200 μm. Reduced channel offsets would further increase the already high measured N/m values.

To further quantify system performance, SR was investigated for on-chip SDS-PAGE carried out at acrylamide gel concentrations of 4%, 6%, and 8%, while all other conditions were kept constant (Figure 2). Variation in the total acrylamide concentration, and hence adjustment of the gel pore size, results in preferential size-based sieving of proteins during SDS-PAGE. As evident in Figure 2, a marked increase in the separation resolution was observed between 4% polyacrylamide gels and higher concentration gels. The 6% gel yielded an SR value of 4.6 ± 0.19 (mean ± standard error, n = 4), while SR was 3.6 ± 0.47 (n = 5) in the 8% case. The reported SR was based on peaks 2 and 5 for both the 6% and 8% gel separations at an elapsed separation time of 6 s. Using the SR

metric, minimum resolvable molecular weight differences of 4.1 kDa and 5.3 kDa are estimated for the 6% and 8% gels, respectively, for the conditions described. Both the 6% and 8% gels resulted in well-resolved separation of all five species in less than 30 s at a detector located 4 mm from the injector.

Theoretically, a gel having a higher total acrylamide concentration should provide more sensitive MW discrimination. The *SR* decrease observed between the 6% and 8% gel separations may be attributed to broadened peaks, especially of the larger MW species (peak 5). Increased sieving of high MW proteins in the 8% gel, may result in more ready detection of heterogeneously-labeled large MW species not discernable in lower concentration gels. Increased *SR* may be achieved by employing increased separation channel lengths, an optimized degree of gel matrix cross-linking, and increased field strengths. The limits and constraints governing each operating parameter dictate system design. Separation channel lengths are typically limited by the minimum necessary signal-to-noise ratio required for analyte detection[36], while the appropriate degree of gel matrix cross-linking is governed by the protein size range of interest. Joule heating sets an upper limit on the applied electric field strength.[37]

Effect of Electric Field on Separations. The applied electric field strength was varied in an attempt to ascertain the most favorable separation conditions for the molecular weight range of interest. Figure 3 presents electropherograms of on-chip SDS-PAGE in the 6% and 8% gels at a variety of applied electric field strengths and shows that proteins elute more rapidly with increased gel porosity and applied field strength, as expected. Baseline separation of all species was accomplished in less than 30 s for the separation

conditions shown in Figure 3. The 6% cross-linked gel showed a maximum *N/m* of 3.97 x 10^5 at the mid-range operating field strength (*E* = 298 V/cm). For the 8% cross-linked gel, a maximum *N/m* value of 4.41 x 10^5 was attained at *E* = 280 V/cm. The time-based separation efficiency, *N/s*, ranged from 119 s^{-1} to 186 s^{-1}. It is important to note that the proximity of the detector to the injection junction resulted in modest *N* values, as compared to those previously reported for non-cross-linked gel SDS-PAGE microsystems.[9, 10] While significantly less efficient than the system reported on by Bousse *et al.*[10], the *N/m* and *N/s* values reported here approximately agree with values obtained by Yao *et al.*[9] for a similar microsystem using non-cross-linked sieving matrices. The *N/m* and *N/s* values obtained using the cross-linked gel sieving structures resulted in ~10x better *N/m* and 50-100x better *N/s* values as compared to those of reported capillary-based systems.[9, 38] As the separation speed and separation length are crucial to this work, high *N/s* and *N/m* values are useful. The detector location enabled rapid identification of well-resolved migrating analytes.

Separation Mechanism of On-chip SDS-PAGE. Validation of the size-based separation mechanism of on-chip SDS-PAGE was investigated by performing a Ferguson analysis on the protein standards. The ability to vary total acrylamide concentration in the cross-linked gels enables quantitative estimates of the free solution mobility and retardation coefficients for SDS-protein complexes. As proposed by Ferguson[39], SDS-PAGE is governed by the linear relationship:

$$\log(m) = \log(m_o) - K_r T \qquad \text{Eq. (1)}$$

where μ (cm^2/Vs) is the analyte mobility, μ_o is the mobility of an SDS-protein complex in free solution, K_r is the retardation coefficient defined by Eq. (1), and T is the total

acrylamide concentration. The retardation coefficient is related to the size of the protein and the sieving quality of the separation matrix; most proteins show increased K_r values as molecular weight increases.[40] As T goes to zero, the first term on the right-hand side of Eq. (1) dominates. In this limit of free solution migration, denatured SDS-protein complexes have a common μ_o, as the charge-to-mass ratio is similar for these complexes. Determination of K_r and μ_o for a protein allows estimation of migration behavior in any gel, thus enabling formulation of a calibration curve for proteins of interest.

The standards were separated in 4%, 6%, 8%, and 10% acrylamide gels. Measurement of the mobility of each species in each of the gels, with all other conditions held constant, yielded a log(μ) *vs*. gel acrylamide concentration relationship as presented in Figure 4A. Linear least-squares fits for each protein standard resulted in acceptable linearity for the conditions investigated ($R^2 > 0.941$). Extrapolation of the linear fits to the limiting case of 0% acrylamide gel concentration revealed an approximately constant logarithm of the mobility for all species considered. In this limit, the mobility approximates the mobility of SDS-protein complexes in free solution. Based on the *y*-intercept of the curves shown in Figure 4, the μ_o is estimated to be between 2.8×10^{-4} cm^2/Vs and 3.6×10^{-4} cm^2/Vs. This μ_o range roughly agrees with those estimated by Gerstner *et al*. using an ultrathin-layer SDS-PAGE system.[41] Agreement between the μ_o values for the different proteins indicates that the free solution mobility of the reduced, denatured, SDS-protein complexes is molecular weight independent and suggests that the separation mechanism resolves species based exclusively upon size.[5] Figure 4B shows the retardation coefficient, K_r, for each linear fit in Figure 4A plotted as a function of the reported

molecular weight of each standard. The resulting calibration curve reveals a linear relationship between the slopes of the lines in Figure 4A and protein molecular weight ($y = 2.2\text{x}10^{-3}x - 0.001$; $R^2 = 0.996$), as would also be expected of a purely sized-based separation mechanism. The K_r values obtained in this analysis are on the same order as those reported by Westerhuis *et al*.[42] In addition, the high correlation coefficient suggests the potential for accurate MW estimation based on the calibration curve. Results of the analysis presented confirm a sized-based separation mechanism for on-chip SDS-PAGE in cross-linked polyacrylamide gels.

Standard Curves and Protein Sizing. Analysis of protein migration in a single acrylamide concentration gel resulted in generation of governing calibration equations relating relative migration to MW for each acrylamide concentration. These standard curves for four gel concentrations are presented in Figure 5. The logarithm of MW for each standard was plotted as a function of the migration of each species (normalized to the estimated free solution mobility, $\mu_o \sim 3.1 \times 10^{-4} \text{cm}^2/\text{Vs}$). The measurements revealed unique slopes for each of the gel concentrations investigated and a high degree of linearity in all cases. Note that the low concentration acrylamide gel (4%) has a slope nearly parallel to the *y*-axis. The steep slope indicates a low degree of preferential sieving in this molecular weight range and, thus, virtually ineffective SDS-PAGE separations. As the acrylamide gel concentration increases, the slopes of the standard curves become shallower. As expected, the larger molecular weight species show the largest mobility decrease as the acrylamide gel concentration is increased. At the exclusion limit, proteins that are larger in size than the pore size of the gel matrix will be excluded from the separation, as those species are unable to enter the gel. The exclusion

limit for the gels investigated in this work can be estimated by considering the limit of zero normalized migration in Figure 5. The estimated size exclusion limits were 22024 kDa, 235 kDa and 110 kDa, and 65 kDa for acrylamide gel concentrations of 4%, 6%, 8%, and 10%, respectively.

Construction of standard curves for each gel composition enables efficient protein sizing for unknown species. Four biologically relevant proteins (a toxin, two growth factors, and a cytokine) were characterized to illustrate the applicability of the on-chip SDS-PAGE method presented in this work. Measurements of the normalized migration distance (or relative migration distance) were made for the proteins by separating each species, along with the molecular weight markers, by on-chip SDS-PAGE in a 6% gel. To obtain normalized migration distance, the absolute migration distance of each unknown was divided by the absolute migration distance of α-lactalbumin. Each of the four unknowns was run individually with the molecular weight standards so as to allow definitive peak identification. The 6% gel exhibited sufficient *SR* to determine relative mobility of proteins in this molecular weight range, yet allowed for rapid separations. The relative migration distance for each unknown was used in conjunction with the calibration equation generated from the 6% gel data in Figure 5 to solve for the unknown logarithm of the molecular weight. Table 2 shows the resulting calculated molecular weights for the fluorescently labeled proteins as compared to the supplier-reported molecular weights of the corresponding unlabeled species. The run-to-run variation in the normalized migration distances and, hence, the variation within the calculated molecular weights for each analyte was small (<10% for all species). The apparent correlation between decreasing MW and increasing deviation between reported and

calculated MW may be attributed to the fact that these smaller proteins are at the lower end of the resolvable protein range expected for a 6% gel. Using a 10% gel, initial estimates of MW for IGF* were ~7.1 kDa. Based upon this observation, Ferguson analysis, including gels consisting of pores smaller than those of the 6% gel, could be employed to analyze the smaller MW proteins.

To demonstrate the applicability of on-chip SDS-PAGE of biologically relevant proteins, a mixture of IGF*, IL-2*, and FGF* was analyzed in a 10% gel. An electropherogram collected 9 mm from the injection junction is presented in Figure 6. IGF*, IL-2*, and FGF* are resolvable, although not baseline separated. Increasing *E* or increasing the separation length could improve the resolution. Even so, all three proteins of interest are identifiable, as are the 29 kDa standard and two impurities (24.8 and 26.8 kDa). The inset in Figure 6 shows a standard curve generated from the normalized mobility (μ/μ_o) of the IGF*, IL-2*, FGF*, and carbonic anhydrase. Molecular weights calculated from the 6% gel calibration equation, as presented in Table 2, were used to generate the IGF*, IL-2*, and FGF* standard curve. A linear least-squares fit to the data from the 10% gel-based separation of the sample species shows a good degree of linearity ($R^2 > 0.984$). The data presented in Figure 6 demonstrate the ability to separate IGF*, IL-2*, and FGF* by on-chip SDS-PAGE in less than 60 s.

Detection Limits and System Reliability. System detection limits were calculated based upon measured signal intensity and the root mean square noise of the background signal for CCD images of TTC* at an elapsed separation time of 10.6 s. Images were collected using a 4x objective with a 400 ms CCD exposure time and 4*x*4 pixel binning.

These conditions were chosen so as to represent typical imaging parameters, yet provide an estimate of the lower limit on sensitivity for this system. Using a critical signal-to-noise ratio of 3, the minimum detectable TTC* concentration was ~20nM. The minimum detectable concentration falls within the expected sensitivity range for the low-magnification imaging system described, and is competitive with other reported on-chip SDS-PAGE systems.[10] Optimization of sensitivity would involve use of a standard laser induced fluorescence system employing a photomultiplier tube for detection. Additionally, the present non-optimized study involves proteins fluorescently labeled off-chip, other recent studies demonstrate the promise of on-chip fluorescent labeling techniques that rely on binding between fluorescent dyes and SDS-protein complexes.[10-12] Incorporation of such techniques would enable relative protein concentration quantitation by eliminating complexities associated with variable protein labeling efficiencies.

Data for the migration behavior of trypsin inhibitor, carbonic anhydrase, and alcohol dehydrogenase in 6% gel-based SDS-PAGE separations was used to ascertain the chip-to-chip reproducibility of the system. Normalized migration distances and run-to-run variation (n = 21 for each analyte) are: 0.88 ± 0.05 for trypsin inhibitor; 0.75 ± 0.05 for carbonic anhydrase; and 0.61 ± 0.05 for alcohol dehydrogenase. The reference protein, α-lactalbumin, had a standard deviation in absolute migration distance of 8% (n=5). Chip-to-chip variation in normalized migration distance was measured to be less than 13% for the three standards between two chips. Calibration runs using protein standards, as are routinely implemented in slab gel SDS-PAGE, are suggested as a method to further improve the chip-to-chip reproducibility. While separation performance was found to

decrease[21, 43] when separations were conducted at high field strengths (>380V/cm) or used for extended periods of time (over 500 separation runs), the measured variation in migration distance indicates acceptable run-to-run and chip-to-chip reproducibility. Further improvements in gel robustness are being pursued in our laboratory.

Conclusions

We have demonstrated *in situ* photopolymerized cross-linked acrylamide gels for SDS-PAGE analysis of proteins in a microdevice format. Microdevice-based protein analysis using a cross-linked sieving matrix was permitted through use of the reported photopolymerization technique. Ferguson analysis confirmed a sized-based protein separation mechanism for SDS-PAGE in the gels, while standard curves provided a means to correlate species' mobility with molecular weight. System performance, quantified through *SR* and efficiency indices, was ample for protein analysis enabling rapid separations of analytes in short separation lengths.

In future work, we plan to integrate the cross-linked gel sieving media into devices capable of parallel analysis of single and multiple sample mixtures. Extension of this work to include gels having spatially varying properties (e.g., gradient porosity gels) and integration of cross-linked gels as components of on-chip multidimensional separation systems are also underway in our laboratory. Development of rapid separation schemes with tunable properties may prove integral to microdevice-based analysis of complex biological samples.

Acknowledgements

The authors thank G.B. Sartor, S.L. Jamison, W.H. Kleist, D.J. Throckmorton, Dr. S.A. Pizarro, and Dr. R. Shediac. This work was financially supported by a grant from the National Institute of Dental and Craniofacial Research (Grant U01DE014961). Sandia is a multi-program laboratory operated by Sandia Corp., a Lockheed Martin Co., for the United States Department of Energy under Contract DE-AC04-94AL85000.

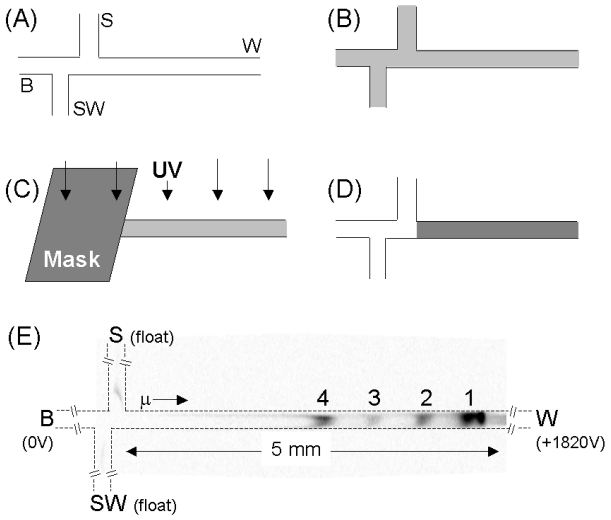

Figure 1. SDS-PAGE using photodefined cross-linked polyacrylamide gel. Photopatterning steps include: (A) conditioned open channels, (B) monomer is flushed into all channels, (C) channels are exposed to a UV source, regions can be optionally masked to prevent cross-linking, and (D) cross-linked polymer is fabricated in non-masked regions. (E) is an inverted grayscale image of an on-chip SDS-PAGE separation at an elapsed separation time of 6.4 s. Sieving matrix is a photolithographically fabricated cross-linked 6% gel patterned in all regions of the microdevice. Proteins: (1) α-lactalbumin, (2) trypsin inhibitor, (3) carbonic anhydrase, and (4) alcohol dehydrogenase. For clarity, microchannel sidewalls have been enhanced and the image aspect ratio has been altered. Separation voltages as indicated, E = 298 V/cm.

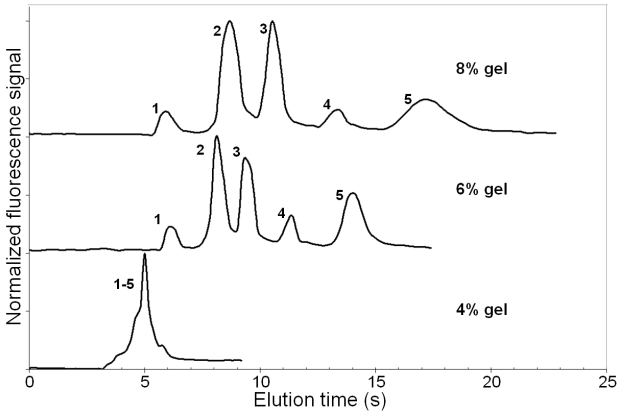

Figure 2. On-chip SDS-PAGE migration behavior as a function of total acrylamide concentration. Electropherograms for SDS-PAGE separations in three gel compositions (4%, 6%, and 8%) are shown. Species are: (1) aprotinin, 6.5kDa; (2) α-lactalbumin, 14.2kDa; (3) trypsin inhibitor, 20.1kDa; (4) carbonic anhydrase, 29kDa; and (5) alcohol dehydrogenase, 39kDa. Length to detector: 4 mm; E = 298 V/cm.

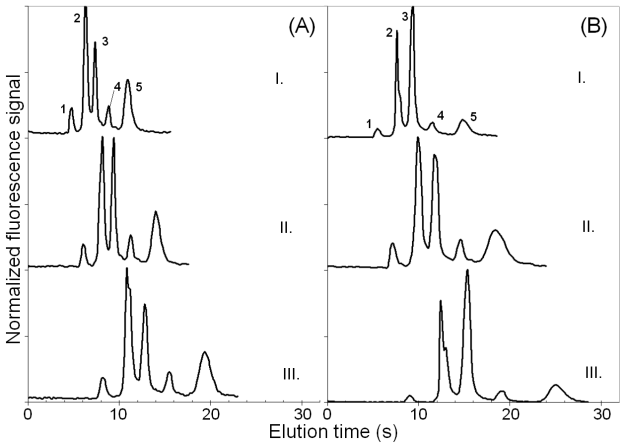

Figure 3. Dependence of migration behavior on gel composition and applied field strength. Electropherograms are shown for (A) 6% and (B) 8% gel concentrations at field strengths of (I) 380 V/cm, (II) 298 V/cm, and (III) 216 V/cm. Species labels correspond to those of Figure 2. Length to detector: 4 mm.

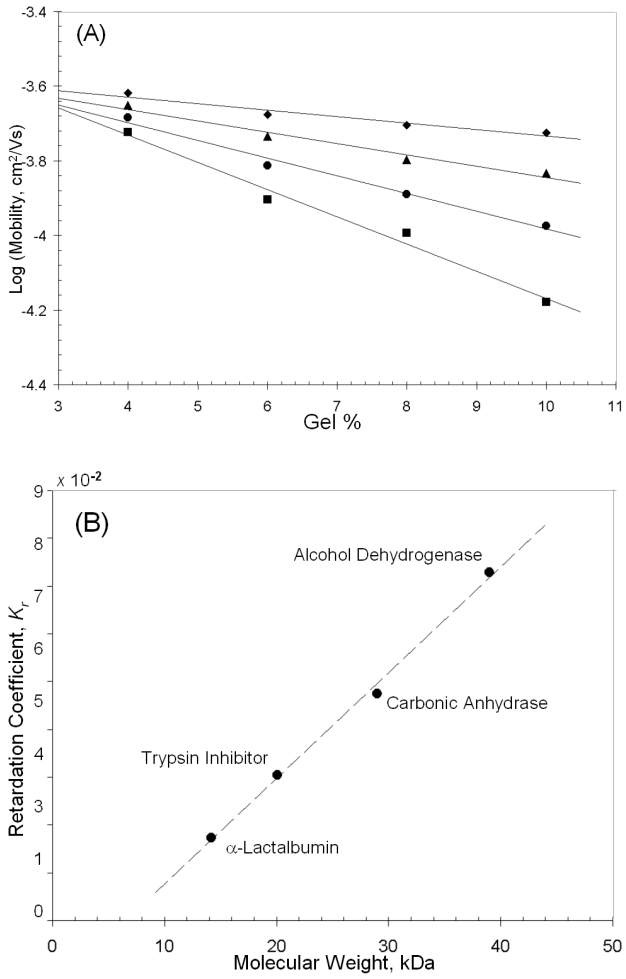

Figure 4. Ferguson and calibration plots for on-chip SDS-PAGE separation of protein standards. (A) Plot of logarithm mobility *vs*. gel composition for (diamonds) α-lactalbumin, K_r = –1.74 x 10^{-2}; (triangles) trypsin inhibitor, K_r = –3.05 x 10^{-2}; (circles) carbonic anhydrase K_r = –4.74 x 10^{-2}; and (squares) alcohol dehydrogenase, K_r = –7.28 x 10^{-2}. (B) Slope information from (A) is formulated in a calibration plot described by the linear relation: $y = 2.2\text{x}10^{-3}x - 0.001$ ($R^2 = 0.9962$). E = 298 V/cm.

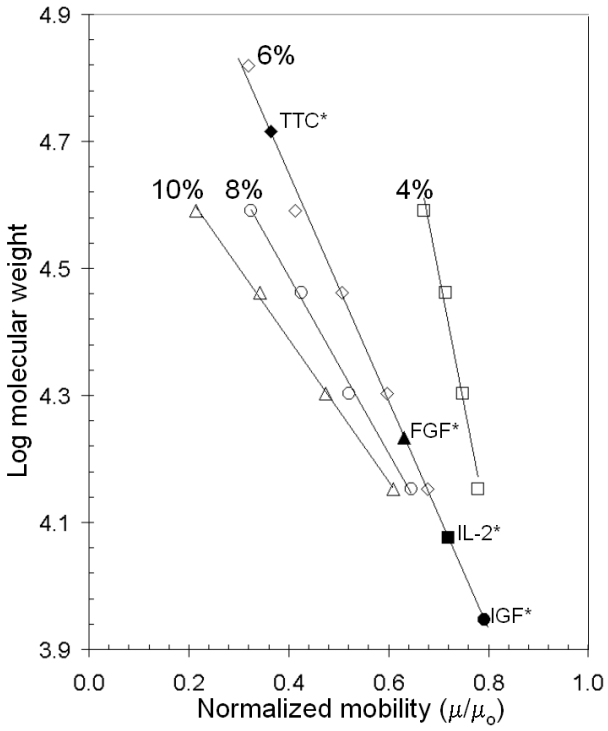

Figure 5. Standard curves of logarithmic molecular weight *vs*. normalized migration for on-chip SDS-PAGE. Standard curves based on molecular weight standards are shown for 4% (hollow squares), 6% (hollow diamonds), 8% gels (hollow circles), and 10% gels (hollow triangles). Measured migration behavior in 6% gels for TTC*, FGF*, IL-2*, IGF* was used with the least-squares linear fit for the 6% gel to calculate the molecular weights of these fluorescently labeled species. Calibration equations: 4% gel: $y = -4.1x + 7.3$ (R^2=0.984); 6% gel: $y = -1.7x + 5.3$ (R^2=0.996); 8% gel: $y = -1.4x + 5.0$ (R^2=0.996); 10% gel: $y = -1.1x + 4.8$ (R^2=0.999). E = 298 V/cm.

	Calculated MW (kDa)	Reported MW (kDa)	Discrepancy (kDa)
(1) TTC	51.9 ± 4.5	51.9	-0.06
(2) FGF	17.0 ± 0.2	17.4	0.24
(3) IL-2	11.8 ± 1.0	15.5	3.62
(4) IGF	8.8 ± 0.8	7.7	-1.21

Table 2. Comparison of measured and reported molecular weights for four protein species. Measured migration behavior and the least squares linear fit presented in Figure 5 for the 6% gel was used to calculate molecular weights for the four fluorescently labeled protein species. Reported MW values were supplier-provided and are for non-fluorescently labeled species.

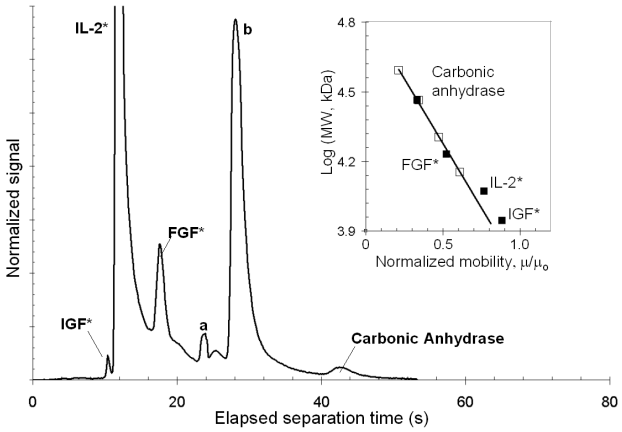

Figure 6. On-chip SDS-PAGE separation of IGF*, IL-2*, and FGF*. An electropherogram for the separation is shown along with an inset showing the standard curve for this separation (solid squares) and the molecular weight standards (hollow squares). The standard curve was generated using the species mobility in the 10% gel normalized to the measured average free solution mobility and the previously measured molecular weights (Table 2). Impurities at (a) 24.9 and (b) 26.9 kDa are resolvable. Conditions: 10% gel; length to detector: 9 mm; E = 298 V/cm..

References

(1) Raymond, S.; Weintraub, L. *Science* **1959**, *130*, 711-711.
(2) Shapiro, A. L.; Vinuela, E.; Maizel, J. V. *Biochem. Biophys. Res. Commun.* **1967**, *28*, 815-&.
(3) Laemmli, U. K. *Nature* **1970**, *227*, 680-&.
(4) Ofarrell, P. H. *Science* **1985**, *227*, 1586-1589.
(5) Cohen, A. S.; Karger, B. L. *J. Chromatogr.* **1987**, *397*, 409-417.
(6) Hjerten, S.; Elenbring, K.; Kilar, F.; Liao, J. L.; Chen, A. J. C.; Siebert, C. J.; Zhu, M. D. *J. Chromatogr.* **1987**, *403*, 47-61.
(7) Zhu, M. D.; Hansen, D. L.; Burd, S.; Gannon, F. *J. Chromatogr.* **1989**, *480*, 311-319.
(8) Widhalm, A.; Schwer, C.; Blaas, D.; Kenndler, E. *J. Chromatogr.* **1991**, *549*, 1-2.
(9) Yao, S.; Anex, D. S.; Caldwell, W. B.; Arnold, D. W.; Smith, K. B.; Schultz, P. G. *Proc. Natl. Acad. Sci. U.S.A.* **1999**, *96*, 5372-5377.
(10) Bousse, L.; Mouradian, S.; Minalla, A.; Yee, H.; Williams, K.; Dubrow, R. *Anal. Chem.* **2001**, *73*, 1207-1212.
(11) Jin, L. J.; Giordano, B. C.; Landers, J. P. *Anal. Chem.* **2001**, *15*, 4994-4999.
(12) Li, Y.; Buch, J. S.; Rosenberger, F.; DeVoe, D. L.; Lee, C. S. *Anal. Chem.* **2004**, *76*, 742-748.
(13) Seiler, K.; Harrison, D. J.; Manz, A. *Anal. Chem.* **1993**, *15*, 1481-1488.
(14) Jacobson, S. C.; Hergenroder, R.; Koutny, L. B.; Ramsey, J. M. *Anal. Chem.* **1994**, *66*, 1114-1118.
(15) Koutny, L. B.; Schmalzing, D.; Taylor, T. A.; Fuchs, M. *Anal. Chem.* **1996**, *68*, 18-22.
(16) Brahmasandra, S. N.; Ugaz, V. M.; Burke, D. T.; Mastrangelo, C. H.; Burns, M. A. *Electrophoresis* **2001**, *22*, 300-311.
(17) Timofeev, E. N.; Kochetkova, S. V.; Mirzabekov, A. D.; Florentiev, V. L. *Nucleic Acids Res.* **1996**, *15*, 3142-3148.
(18) Guschin, D.; Yershov, G.; Zaslavsky, A.; Gemmell, A.; Shick, V.; Proudnikov, D.; Arenkov, P.; Mirzabekov, A. *Anal. Biochem.* **1997**, *1*, 203-211.
(19) Proudnikov, D.; Timofeev, E.; Mirzabekov, A. *Anal. Biochem.* **1998**, *15*, 34-41.
(20) Vasiliskov, A. V.; Timofeev, E. N.; Surzhikov, S. A.; Drobyshev, A. L.; Shick, V. V.; Mirzabekov, A. D. *Biotechniques* **1999**, *27*, 592-+.
(21) Olsen, K. G.; Ross, D. J.; Tarlov, M. J. *Anal. Chem.* **2002**, *15*, 1436-1441.
(22) Yu, C.; Svec, F.; Frechet, J. M. J. *Electrophoresis* **2000**, *21*, 120-127.
(23) Shediac, R.; Ngola, S. M.; Throckmorton, D. J.; Anex, D. S.; Shepodd, T. J.; Singh, A. K. *J. Chromatogr. A* **2001**, *3*, 1-2.
(24) Throckmorton, D. J.; Shepodd, T. J.; Singh, A. K. *Anal. Chem.* **2002**, *74*, 784-789.
(25) Han, J. Y.; Singh, A. K. *Proceedings of the uTAS 2002 Symposium*, Nara, Japan 2002; Kleuwer Academic Publishers.; 596-598.
(26) Shediac, R.; Pizarro, S. A.; Herr, A. E.; Singh, A. K. *Proceedings of the uTAS 2003 Symposium*, Squaw Valley, CA USA, October 5-9 2003; Transducers Research Foundation; 971-974.
(27) Schwartz, H.; Palmieri, R.; Brown, R.; CRC Press: Boca Raton, FL, 1993.
(28) Rocklin, R. D.; Ramsey, R. S.; Ramsey, J. M. *Anal. Chem.* **2000**, *72*, 5244-5249.
(29) Gottschlich, N.; Jacobson, S. C.; Culbertson, C. T.; Ramsey, J. M. *Anal. Chem.* **2001**, *73*, 2669-2674.
(30) Herr, A. E.; Molho, J. I.; Drouvalakis, K. A.; Mikkelsen, J. C.; Utz, P. J.; Santiago, J. G.; Kenny, T. W. *Anal. Chem.* **2003**, *1*, 1180-1187.
(31) Li, Y.; Buch, J. S.; Rosenberger, F.; DeVoe, D. L.; Lee, C. S. *Anal Chem* **2004**, *76*, 742-748.
(32) Helting, T. B.; Zwisler, O. *J. Biol. Chem.* **1977**, *252*, 187-193.
(33) Kirby, B. J.; Wheeler, A. R.; Zare, R. N.; Fruetel, J. A.; Shepodd, T. J. *Lab Chip* **2003**, *3*, 5-10.
(34) Giddings, J. C. *Unified Separation Science*; John Wiley and Sons: New York, 1991.
(35) Jacobson, S. C.; Hergenroder, R.; Koutny, L. B.; Warmack, R. J.; Ramsey, J. M. *Anal. Chem.* **1994**, *66*, 1107-1113.
(36) Bharadwaj, R.; Santiago, J. G.; Mohammadi, B. *Electrophoresis* **2002**, *23*, 2729-2744.
(37) Grushka, E.; McCormick, R. M.; Kirkland, J. J. *Anal. Chem.* **1989**, *61*, 241-246.
(38) Wise, E. T.; Singh, N.; Hogan, B. L. *J. Chromatogr. A* **1996**, *4*, 109-121.
(39) Ferguson, K. A. *Metabolism* **1964**, *13*, 985-&.
(40) Rodbard, D.; Chrambach, A. *Anal. Biochem.* **1971**, *40*, 95-&.
(41) Gerstner, A.; Csapo, Z.; Sasvari-Szekely, M.; Guttman, A. *Electrophoresis* **2000**, *21*, 834-840.
(42) Westerhuis, W. H. J.; Sturgis, J. N.; Niederman, R. A. *Anal. Biochem.* **2000**, *15*, 143-152.

(43) Zangmeister, R. A.; Tarlov, M. J. *Langmuir* **2003**, *19*, 6901-6904.